Theory of Spin Susceptibility in Frustrated Layered Antiferromagnets

A.F. Barabanov,* A.V. Mikheyenkov, and A.M. Belemuk
Institute for High Pressure Physics, Russian Academy of Sciences, Troitsk 142190, Moscow Region, Russia
(Dated: February 6, 2008)

The self-consistent treatment of real and imaginary renormalizations in the dynamic spin susceptibility $\chi(\mathbf{q},\omega)$ for the frustrated Heisenberg model reproduces for cuprates at low doping: a spin spectrum $\omega_{\mathbf{q}}$, a saddle point for $\mathbf{q} \approx (\pi/2,\pi/2)$, nearly constant q-integrated susceptibility $\chi_{2D}(\omega)$ for $\omega \lesssim 150\,meV$ and a scaling law for $\chi_{2D}(\omega)$. Frustration increase (optimally doped case) leads to a stripe scenario with an $\omega_{\mathbf{q}}$-saddle point at $\mathbf{q} \approx(\pi;\pi/2)$ and $\chi_{2D}(\omega)$ peak at $\omega \approx 30\,meV$. The obtained $\chi(\mathbf{q},\omega)$ describes neutron scattering results and leads to well-known temperature transport anomalies in doped cuprates.

PACS numbers: 74.72.-h, 71.27.+a, 75.20.-g

The investigation of the dynamic spin susceptibility $\chi(\mathbf{q},\omega)$ is a key problem for understanding the physics of layered high-T_c superconductors (HTSC) in both low and optimally doped regimes. The inelastic neutron scattering (INS) measurements in cuprates [1] – [3] revealed a sharp resonant magnetic excitations peak of $\chi^{''}(\mathbf{q},\omega) = Im\chi(\mathbf{q},\omega)$ which corresponds to the aniferromagnetic (AFM) wave vector $\mathbf{Q} = (\pi,\pi)$ at a resonant energy $E_r \approx 30\,meV$ and a low-temperature peak at close energies for q-integrated susceptibility $\chi_{2D}(\omega,T)$, $\chi_{2D}(\omega,T) = \int d\mathbf{q}\chi^{''}(\mathbf{q},\omega,T)$. At low doping INS demonstrates the scaling of magnetic response – the universal law for $\chi_{2D}(\omega,T)$ [4] which states

$$\frac{\chi_{2D}(\omega,T)}{\chi_{2D}(\omega,T\to 0)} = f(\omega/T) \qquad (1)$$

In the mentioned regime the spin excitation dispersion $\omega(\mathbf{q})$ was measured across the entire Brillouin zone [13] and it was found that $\omega(\mathbf{q})$ is anisotropic around the magnetic zone boundary (a saddle point at $\mathbf{q} \approx(\pi,\pi/2)$).

The aim of the work is to present a theory for the dynamic spin susceptibility $\chi(\mathbf{q},\omega)$ within the frustrated $S = 1/2$ Heisenberg model taking into account real and imaginary renormalizations extracted from the irreducible Green's function $M(\mathbf{q},\omega)$ so as to describe the mentioned experimental results in both doping regimes in the framework of one self-consistent approach. Our analysis is based on a spherically-symmetric treatment of the spin system which was introduced by Shimahara and Takada [8] and generalized in [9].

The recent microscopic theoretical progress in the investigations of $\chi(\mathbf{q},\omega)$ [5, 6, 7] is based on $t-J$ model treated within the memory function approach (MFA). This approach demonstrates $\chi^{''}(\mathbf{Q},\omega)$ peaks and the scaling law. It is close to our treatment but it has difficulties in an analytical calculation of the explicit form for $\omega(\mathbf{q})$ and a spin gap and as a result in the self-consistency procedure. Relative to MFA our theory gives such new results as a demonstration of $\omega(\mathbf{q})$ – saddle point at $\mathbf{q} \approx(\pi;\pi/2)$ and a new analytical form for a scaling law for small frustration case (strongly underdoped regime). For the large frustration (the regime close to optimal doping) we reproduce not only $\chi^{''}(\mathbf{Q},\omega)$ peaks, but also the peaks of $\chi_{2D}(\omega)$ demonstrating a stripe scenario (see [2] for a review). For the latter case we calculate also the resistivity $\rho(T)$ and the Hall coefficient $R(T)$ in order to be sure that the found $\chi(\mathbf{q},\omega)$ reproduces the well-known temperature anomalies in kinetics.

The Hamiltonian of the model has the form

$$\widehat{H}_I = \frac{1}{2}I_1\sum_{\mathbf{i},\mathbf{g}}\overrightarrow{\mathbf{S}}_{\mathbf{i}}\overrightarrow{\mathbf{S}}_{\mathbf{i+g}} + \frac{1}{2}I_2\sum_{\mathbf{i},\mathbf{d}}\overrightarrow{\mathbf{S}}_{\mathbf{i}}\overrightarrow{\mathbf{S}}_{\mathbf{i+d}} \qquad (2)$$

It describes the frustrated system of localized $S = 1/2$ spins on a square lattice, where I_1 is an AFM interaction constant for nearest, I_2 – for next-nearest neighbors, $\mathbf{g},\mathbf{d}$ – vectors of nearest and next-nearest neighbors. We use standard variable p ("frustration parameter") $p = I_2/I$, $I_1 = (1-p)I$, $I_2 = pI$, $I = I_1 + I_2$ as a measure of frustration, hereinafter we treat all the energetic parameters in the units of I and put $I = 1$. We suppose that the frustration (term I_2) simulates the influence of doping.

Following [8, 9, 10] we calculate $\chi(\mathbf{q},\omega) = -\langle\langle S^\alpha_{\mathbf{q}} \mid S^\alpha_{-\mathbf{q}}\rangle\rangle_\omega$ – two-time retarded Green's function by the irreducible Green's function method. The dynamic spin susceptibility can be written as $\chi(\mathbf{q},\omega) = -F_{\mathbf{q}}/(\omega^2 - \omega^2_{\mathbf{q}} - M(\mathbf{q},\omega))$, where $\omega_{\mathbf{q}}$ is the spin excitations spectrum, $M(\mathbf{q},\omega) = M^{'} + iM''$ – Fourier-transform of a new complex three-site irreducible retarded Green's function, its analytical properties are the same as those of $\chi(\mathbf{q},\omega)$.

Spectrum $\omega_{\mathbf{q}}$ and the numerator $F_{\mathbf{q}}$ have a cumbersome form but they are expressed explicitly over five spin-spin correlation functions $c_{\mathbf{g}}, c_{\mathbf{d}}, c_{\mathbf{g+g}}, c_{\mathbf{d+d}}, c_{\mathbf{g+d}}$ [9], $c_{\mathbf{r}} = \langle S^\alpha_{\mathbf{R}} S^\alpha_{\mathbf{R+r}}\rangle = (2\pi)^{-2}\int d\mathbf{q}\, c_{\mathbf{q}} e^{i\mathbf{qr}}$. This allows to write down and solve numerically self-consistent system through the usual relations $c_{\mathbf{q}} = \langle S^z_{\mathbf{q}} S^z_{-\mathbf{q}}\rangle = -\pi^{-1}\int d\omega\, n_B(\omega) Im\langle\langle S^\alpha_{\mathbf{q}} \mid S^\alpha_{-\mathbf{q}}\rangle\rangle_{\omega+i\delta}$, $S^\alpha_{\mathbf{q}} = N^{-1/2}\sum_{\mathbf{q}} e^{-i\mathbf{qr}} S^\alpha_{\mathbf{r}}$. The set of equations includes also the sum-rule condition $c_{\mathbf{r=0}} = 1/4$. The system is solved at every fixed T and p.

*Electronic address: abarab@bk.ru

The imaginary part $M''(\mathbf{q},\omega)$ is an odd function of ω. In the simplest approach [5] we put $M''(\mathbf{q},\omega) = -\omega\gamma$, where the damping γ is taken to be independent on $\mathbf{q}$ and ω. We take the real part $M^{'}$ as $M^{'} \sim |\sin(q_x)\sin(q_y)|^3$ and introduce a renormalized spectrum $\widetilde{\omega}^2_{\mathbf{q}} = \omega^2_{\mathbf{q}} + (\lambda|\sin q_x \sin q_y|)^3$. The choice of $M^{'}$functional form is dictated by the condition that $M^{'}$ represents the square harmonic different from those involved in the functional form of $\omega^2(\mathbf{q})$. Though the λ-renormalization is zero along the lines $\mathbf{\Gamma}-\mathbf{X}$ and $\mathbf{X}-\mathbf{M}$ ($\mathbf{\Gamma}=(0,0)$, $\mathbf{X}=(0,\pi)$, $\mathbf{M}=(\pi,\pi)$) and mainly modifies the top of the spectrum, it changes the spin gap $\Delta_{\mathbf{M}} = \widetilde{\omega}_{\mathbf{Q}}$ due to self-consistency of calculations. So the dynamic spin susceptibility

$$\chi(\mathbf{q},\omega) = \frac{-F_{\mathbf{q}}}{\omega^2 - \widetilde{\omega}^2_{\mathbf{q}} + i\omega\gamma}, \qquad (3)$$

contains two parameters γ and λ.

We relate the dielectric limit to the case of extremely small frustration $p = 0.04$. In the inset of Fig.1 the spectrum $\widetilde{\omega}(\mathbf{q})$ is presented in this limit for $T = 0.1$, $\gamma = 0.025$ and $\lambda = -1.0$ ($T \sim 100K$ for $I \sim 100\,meV$). The spectrum is almost linear on $\widetilde{q} = |\mathbf{q}-\mathbf{Q}|$ up to $\omega_0 \sim 1.5$. It can be found that for fixed $\mathbf{q}$ there is a well-defined $\chi(\mathbf{q},\omega)$ peak on ω which is related to the spectrum $\widetilde{\omega}(\mathbf{q})$. More exactly, the maximum of $\chi(\mathbf{q},\omega)$ on ω corresponds to the frequency close to $\widetilde{\omega}(\mathbf{q})$, but always a bit smaller (due to damping γ). For $I = 1.2\,meV$ a spin-wave velocity $\hbar c \approx 900\ meV\,\AA$ is close to the value given in [11]. As it is seen from the inset of Fig.1, in accordance with the experiments [13], the dispersion $\widetilde{\omega}(\mathbf{q})$ is anisotropic around the magnetic zone boundary and has a saddle point close to $\mathbf{q} = \mathbf{Q}/2$ ($\widetilde{\omega}(\mathbf{q}=(0,\pi) > \widetilde{\omega}(\mathbf{q}=(\pi/2,\pi/2))$). Note that in contrast to our treatment one needs to adopt a ferromagnetic second-neighbor exchange I_2 with $p \leq -0.1$ for the explanation of such an anisotropy in the framework of the linear spin-wave theory [13].

In Fig.1 $\chi_{2D}(\omega)$ is given for $p = 0.04$, $\gamma = 0.25T$ in two cases: $T = 0.1$, $\lambda = -1.0$ and $T = 0.3$, $\lambda = 2.0^{1/3}$. The λ-values are chosen from the condition that the resulting spin gap should be approximately linear on T : $\Delta_{\mathbf{M}}(T = 0.1) = 0.048$, $\Delta_{\mathbf{M}}(T = 0.3) = 0.134$. Below we show analytically that in the low-frustration limit this linearity is the necessary condition for the scaling law. The qualitative coincidence of calculated function with the experiment [11, 12] is seen – $\chi_{2D}(\omega)$ is nearly constant in a large ω interval and increases for $\omega > 150\,meV$.

Now we treat the scaling condition which leads to a strong limitation of $\gamma(T)$ dependence. Fig.2 represents the scaling functions $f(\omega/T)$. Solid lines **b** and **c** correspond to temperatures $T = 0.1$ and $T = 0.3$ respectively and are calculated for the same parameters, as in Fig.1 (that is, in particular, for $\gamma = 0.25T$). The dash-dotted line **a** is the best fit for experimental scaling in $La_{1.96}Sr_{0.04}CuO_4$ [4] $f_{ex}(\omega/T) = (2/\pi)\arctan\{0.43(\omega/T) + 10.5(\omega/T)^3\}$. It is approximately a step function on (ω/T) smeared through $\delta = \Delta(\omega/T) \simeq 0.25$. The calculated curves have close value of δ. Note that the value of δ strongly restricts the $\gamma(T)$ dependence. For example, thin curve **d** in Fig.2 corresponds to $T = 0.3$, $\lambda = 2.0^{1/3}$ and $\gamma = 0.3 > 0.25T = 0.075$. As a result curve **d** strongly deviates from curves **a** (f_{ex}) and **c** ($f_{T=0.3,\gamma=0.25T}$) and it has $\delta \gg 0.25$.

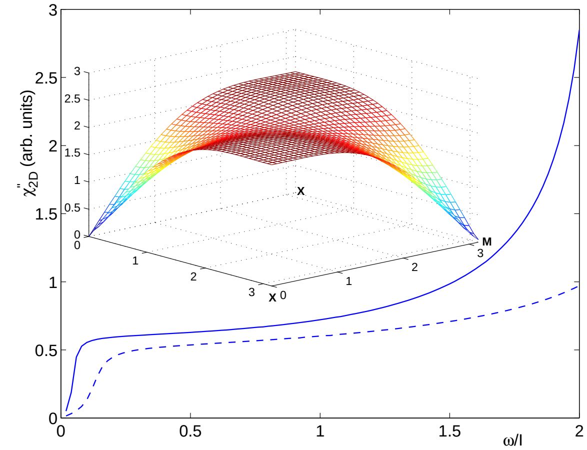

FIG. 1: $\chi_{2D}(\omega)$ for frustration $p = 0.04$: $T/I = 0.1$ – solid, $T/I = 0.3$ – dashed curve (damping $\gamma = 0.5T$). *Inset*: self-consistent spectrum $\widetilde{\omega}(\mathbf{q})$ for $p = 0.04$ and $T/I = 0.1$

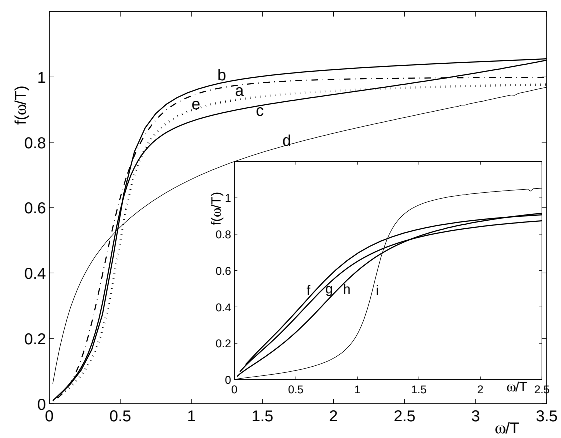

FIG. 2: Scaling curves $f(\omega/T)$ for $p = 0.04$: the dashed-dotted line **a** – best fit for scaling in $La_{1.96}Sr_{0.04}CuO_4$ [4]; solid lines **b** and **c** were calculated at $T/I = 0.1$; 0.3 for $\gamma = 0.25T$; dotted line **e** – scaling law (4) – see text; solid thin curve **d**– destroyed scaling $T = 0.3$ and $\gamma/I = 0.3 > 0.25T/I = 0.075$. *Inset*: Scaling for $p = 0.1$: solid curves **f**,**g**,**h** respectively for $T/I = 0.1$;0.2;0.4, $\gamma = T$. The solid thin curve **l** – $T/I = 0.4$ and $\gamma/I = 0.1 < T/I = 0.4$.

The analogous picture for the frustration $p = 0.1$ is shown in the inset of Fig.2 for $\gamma = T$ and $\lambda = 0$ We relate this case to strongly underdoped Y**-**cuprates [14]. The calculated scaling functions are given for the temperatures $T = 0.1, 0.2, 0.4$ by the solid curves **f**, **g**, **h**

respectively. It can be seen that they are close to the experimental $f_{ex}(\omega/T) = (\frac{2}{\pi})\arctan\{a(\omega/T)\}$, $a \sim 1$ [14]. The thin curve **l** corresponds to $T = 0.4$ and $\gamma = 0.1 < T = 0.4$. Comparison of the curves **h** and **l** explicitly demonstrates that, as in the previous case $p = 0.04$, the scaling is destroyed when $\gamma(T)$ deviates from a linear law.

Thus, the above results demonstrate that the scaling law holds if γ is a linear function on T. In the limit $p \ll 1$ this point can be clarified analytically taking $Im\chi(\mathbf{q},\omega) = \gamma\omega F_{\mathbf{q}}/\{(\omega^2-\omega_{\mathbf{q}}^2)^2+\gamma^2\omega^2\}$ It is obvious from the inset of Fig.1 that for $\omega/T \le 2$, $T/I \le 0.3$ the main input to $\chi_{2D}(\omega)$ is given by the region $\widetilde{q} \le \widetilde{q}_0$; $c\widetilde{q}_0 \sim I$ is the largest energetic parameter. Then $\omega^2(q) \approx \Delta_{\mathbf{M}}^2 + c^2\widetilde{q}^2$ and simple integration gives for $\omega < c\widetilde{q}_0$

$$\chi_{2D}(\omega) = \frac{\overline{F_{\mathbf{q}}}}{4\pi c^2}\left[\begin{array}{ll} \Phi(\omega,\Delta_{\mathbf{M}},\gamma); & for\ \theta < 1 \\ \pi + \Phi(\omega,\Delta_{\mathbf{M}},\gamma); & for\ \theta > 1 \end{array}\right] \quad (4)$$

$$\begin{aligned} \theta &= (c^2\widetilde{q}_0^2 + \Delta_{\mathbf{M}}^2 - \omega^2)(\omega^2 - \Delta_{\mathbf{M}}^2)/\gamma^2\omega^2 \\ \Phi &= \arctan\left\{\frac{c^2\widetilde{q}_0^2\gamma\omega}{\gamma^2\omega^2 + (c^2\widetilde{q}_0^2 + \Delta_{\mathbf{M}}^2 - \omega^2)(\Delta_{\mathbf{M}}^2 - \omega^2)}\right\} \end{aligned}$$

Here $\overline{F_{\mathbf{q}}}$ is the averaged smooth function $F_{\mathbf{q}}$.

In the limit under consideration the scaling denominator $\chi_{2D}(\omega, T \to 0)$ is almost constant in a wide ω-range and scaling is ruled by $\chi_{2D}(\omega,T)$. Accepting in (4) linear $\gamma = \alpha T$ and $\Delta_{\mathbf{M}} = \beta T$ one obviously gets the scaling ($\chi_{2D}(\omega,T)$ becomes $\chi_{2D}(\omega/T)$). So in the mentioned approximations the scaling function can be written as

$$\widetilde{f}(\frac{\omega}{T}) = \pi\Theta((\frac{\omega}{T})^2 - \beta^2) + \arctan\left\{\frac{\alpha(\omega/T)}{(\beta^2 - (\omega/T)^2)}\right\} \quad (5)$$

In contrast to numerous experimental fittings by simple arctan, the scaling function $\widetilde{f}(\omega/T)$ (5) is described by 'switched' arctan law and contains a microscopic information on $\Delta_{\mathbf{M}}$ and γ. The switching by Θ-function takes place at $\omega = \Delta_{\mathbf{M}}$.

In Fig.2 $\widetilde{f}$ is represented for $\alpha = 0.25, \beta = 0.5$ by dotted line **e** and it coincides with $f_{T=0.2,\gamma=0.05}$. The scaling function $\widetilde{f}(\omega/T)$ with slightly different parameters $\alpha = 0.25, \beta = 0.43$ is almost indistinguishable from experimental $f_{ex}(\omega/T)$ [4]. Let us remind, that in the above calculations we have taken $\gamma \sim T$ and such $\lambda(T)$ that the self-consistent calculations led to $\Delta \sim T$.

So in the dielectric limit (small p) the model leads to an adequate description of experimental results. The scaling law strongly restricts $\gamma(T)$ dependence.

Now we turn to the case $p = 0.28$ which corresponds to $\Delta_{\mathbf{M}} \approx \Delta_{\mathbf{X}} = \widetilde{\omega}_{\mathbf{q}=\mathbf{X}}$. We relate this case to the optimal doping. Calculated data are presented for $T = 0.025$ and 0.05 with $\gamma = 0.38 + 0.8T$ (in contrast to low frustration limit here γ does not tend to zero at $T \to 0$) and $\lambda = 10.0^{1/3}$. For $T = 0.025$ and 0.05 the gaps are $\Delta_{\mathbf{M}} = 0.197$, $\Delta_{\mathbf{X}} = 0.179$ and $\Delta_{\mathbf{M}} = 0.228$, $\Delta_{\mathbf{X}} = 0.210$.

Fig.3 shows the Q-peaks, i.e. $\chi''(\mathbf{Q},\omega)$, for $T = 0.025$ and $T = 0.05$. They are also in good agreement with

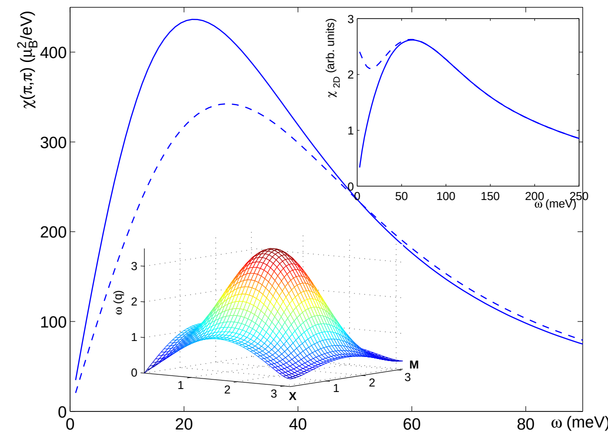

FIG. 3: $\chi''(\mathbf{Q},\omega)$ for $T/I = 0.025$ (solid) and $T/I = 0.05$ (dashed curve) *Inset*: $\chi_{2D}(\omega)$ – solid line and $\chi_{2D}(\omega)(2n_{Bose}+1)$ – dashed line for $T/I = 0.05$; *Lower inset*: The spectrum $\widetilde{\omega}_{\mathbf{q}}/I$ for $p = 0.28$, $T/I = 0.05$.

the experiment [16]. In the inset of Fig.3 the calculated spectrum $\widetilde{\omega}_{\mathbf{q}}$ is shown for $T = 0.05$. The dispersion $\widetilde{\omega}(\mathbf{q})$ has the following new features: the saddle points close to $\mathbf{q} = (\pi;\pi/2); (\pi/2;\pi)$ and $\widetilde{\omega}(\mathbf{q})$ changes weakly along $\mathbf{X}-\mathbf{M}$ direction. That is why $\chi_{2D}(\omega)$ has a peak at $\omega \gtrsim 2 \div 3\,\Delta_{\mathbf{M}}$. This is explicitly seen in the another inset of Fig.3 which gives $\chi_{2D}(\omega)$ (solid line) and $\chi_{2D}(\omega)(2n_{Bose}+1)$ (dashed line) for $T = 0.05$. These curves qualitatively correspond to the experimental ones [15] for optimally doped curates. It is clear that the shown behavior of $\widetilde{\omega}(\mathbf{q})$ and $\chi_{2D}(\omega)$ is a result of a stripe scenario if we remind that the increase of p drives the system to a state which is close to a coherent superposition of two semiclassical stripe phases with $\Delta_{\mathbf{X}} = 0$ [9]. It can be shown that $c_{\mathbf{q}} = \left\langle S^z_{\mathbf{q}} S^z_{-\mathbf{q}}\right\rangle$ is qualitatively different for small and large frustrations. For $p \le 0.1$ the structure factor $c_{\mathbf{q}}$ has an extremely narrow peak at $\mathbf{q} = \mathbf{Q}$. For $p = 0.28$ the structure factor has peaks at $\mathbf{q} = \mathbf{Q} = \mathbf{M}$ and at $\mathbf{q} = \mathbf{X}$. With p increase the peaks at $\mathbf{X}$ points increase and the $\mathbf{M}$ -peak disappears.

We capture this physics taking a spin-only model. But this model is too simple to reflect a well-known low-energy incommensurate magnetic excitations at wave vectors close to $\mathbf{Q}$ at optimal doping. It is obvious that one needs to introduce explicitly the spin-hole scattering to describe this feature.

To check the applicability of the obtained spin susceptibility $\chi(\mathbf{q},\omega)$ for the kinetics of the optimally doped HTSC we calculate the in-plane resistivity $\rho(T)$ and the Hall coefficient $R_H(T)$ in the framework of the spin-fermion model with the Hamiltonian

$$\begin{aligned} \hat{H} &= \hat{H}_0 + \hat{H}_I \qquad (6) \\ \hat{H}_0 &= \sum_{\mathbf{k},\sigma} \varepsilon_{\mathbf{k}} a^\dagger_{\mathbf{k}\sigma} a_{\mathbf{k}\sigma} + J\frac{1}{\sqrt{N}} \sum_{\mathbf{k},\mathbf{q},\gamma_1,\gamma_2} a^\dagger_{\mathbf{k}+\mathbf{q},\gamma_1} S^\alpha_{\mathbf{q}} \hat{\sigma}^\alpha_{\gamma_1\gamma_2} a_{\mathbf{k},\gamma_2} \end{aligned}$$

The hole spectrum $\varepsilon_{\mathbf{k}}$ is obtained from the calculation of

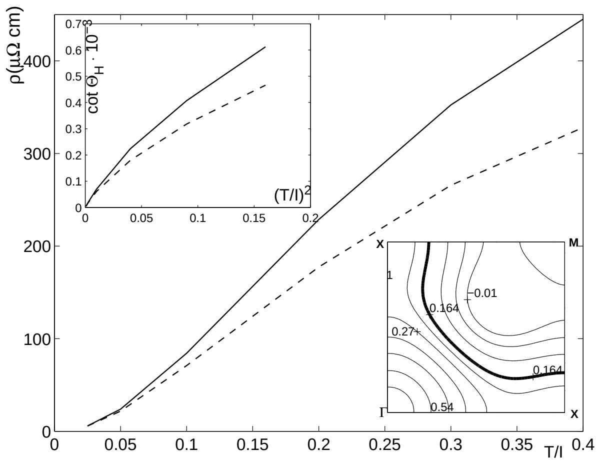

FIG. 4: The resistivity $\rho(T/I)$ and cotangent of the Hall angle $cot\,\Theta_H(T^2/I^2)$ at 10 T (*upper inset*). The solid lines – for $\chi(\mathbf{q},\omega)$ (3). The dashed lines – for overdamped $\chi_{ovd}(\mathbf{q},\omega)$. *Lower inset*: the spectrum $\varepsilon_{\mathbf{k}}$ (in eV) given by the curves $\varepsilon_{\mathbf{k}} = \text{const}$; bold curve – Fermi line for optimal doping.

the lower spin-polaron band in a six pole approximation [17] and is shown in the inset of Fig.4.

It is well known that scattering by the spin-fluctuations with momenta $\mathbf{Q}$ leads to a strongly T-dependent anisotropy. To take it into account the equation of motion for the non-equilibrium density matrix $\hat{\rho}^{(1)} = Z^{-1}\exp(-\hat{H}_0/T)\hat{F}$ is solved by seven-moment approach $\hat{F} = \sum_{l=1\div 7}\eta_l \hat{F}_l$, $\hat{F}_l = \sum_{\mathbf{k},\sigma} F_l(\mathbf{k}) a^{\dagger}_{\mathbf{k}\sigma} a_{\mathbf{k}\sigma}$. The moments $F_l(\mathbf{k})$ are taken to be polynomials in velocity components $\mathbf{v_k} = \partial\varepsilon_{\mathbf{k}}/\hbar\partial\mathbf{k}$ and their derivatives: $F_l^E(\mathbf{k}) = \{v^x_{\mathbf{k}},\, (v^y_{\mathbf{k}})^2 v^x_{\mathbf{k}},\, \frac{\partial v^x_{\mathbf{k}}}{\partial y} v^y_{\mathbf{k}},\, \frac{\partial v^y_{\mathbf{k}}}{\partial y} v^x_{\mathbf{k}},\, \frac{\partial v^x_{\mathbf{k}}}{\partial x}\frac{\partial v^y_{\mathbf{k}}}{\partial y} v^x_{\mathbf{k}},\, (v^x_{\mathbf{k}})^3, \frac{\partial v^x_{\mathbf{k}}}{\partial x} v^x_{\mathbf{k}}\}$.

The detailed expressions for $\rho(T)$ and $R_H(T)$ are given in [18]. The susceptibility $\chi(\mathbf{q},\omega)$ (3) is involved in scattering integrals. To clarify the importance of the form (3) we also present the results for widely used so-called overdamped susceptibility $\chi_{ovd}(\mathbf{q},\omega)$ (when ω^2 term in the denominator of (3) is omitted) [19, 20].

The results presented in Fig.4 are obtained for $p = 0.28$, $I = 100\ meV$ and $J = 200\ meV$. The plots are the resistivity $\rho(T)$ and the Hall angle cotangent $cot\,\Theta_H = \rho_{xx}/(R_H B)$ (in the inset) obtained for the $\chi(\mathbf{q},\omega)$ (3) – solid lines and for $\chi_{ovd}(\mathbf{q},\omega)$ – dashed lines. In accordance with the experiment [21], the $\rho(T)$ curve exhibits a temperature dependence close to a linear one starting from low T with the value $\rho(400K)/\rho(100K) \approx 5$. It can be shown that $\chi_{ovd}(\mathbf{q},\omega)$ approximation underestimates the scattering for large ω. As a result at $\rho(T)_{ovd} < \rho(T)$ and, as it is seen from Fig 4, in some temperature regions $\rho(T)_{ovd}$ has a different curvature. The $cot\,\Theta_H$ exhibits nearly linear behavior on T^2 in a wide temperature range, however, at low temperatures deviation from linearity is obvious. It seems hopeful that the self-consistent spin susceptibility $\chi(\mathbf{q},\omega)$ allows to describe experimental temperature anomalies of two kinetic coefficients simultaneously.

In summary, we have made a systematic self-consistent study of the spin problem in 2D frustrated Heisenberg antiferromagnet. Key features of the model – temperature dependence of the damping in low frustration limit and the appearance of saddle points of the dispersion $\widetilde{\omega}(\mathbf{q})$ close to $\mathbf{q} = (\pi;\pi/2);(\pi/2;\pi)$ in the case of strong frustration increase – allow to relate the results to a wide hole doping interval in cuprates.

Work was supported by Russian Fund of Fundamental Investigations and Russian Science Support Foundation.

[1] P. A. Lee, N. Nagaosa, and X.-G. Wen, Rev. Mod. Phys. **78**, 17 (2006).
[2] R. J. Birgeneau *et al.*, cond-mat/0604667 (2006).
[3] B. Lake *et al.*, Nature **400**, 43 (1999).
[4] B. Keimer *et al.*, Phys. Rev. B **46**, 14034 (1992).
[5] P. Prelovsek, I. Sega and J. Bonca, Phys. Rev. Lett. **92** 027002 (2004).
[6] I. A. Larionov, Phys. Rev. B **72**, 094505 (2005).
[7] A. Sherman, and M. Schreiber, Phys. Rev. B **68**, 094519 (2003).
[8] H. Shimahara, and S. Takada, J. Phys. Soc. Jpn. **60**, 2394 (1991).
[9] A. F. Barabanov, and V. M. Berezovsky, Phys. Lett. A **186**, 175 (1994); JETP **79**, 627 (1994); J. Phys. Soc Jpn. 63 (1994) 3974.
[10] A. F. Barabanov, L. A. Maksimov, Phys. Lett. **A207**, 390 (1995).
[11] S. M. Hayden *et al.*, Phys. Rev. Lett. **76**, 1344 (1996).
[12] S.M. Hayden, G. Aeppli, T.G. Perring, H.A. Mook, F. Dogan, Phys. Rev. B **54**, R6905 (1996).
[13] R. Coldea *et al.*, Phys. Rev. Lett. **86**, 5377 (2001).
[14] C. Stock *et al.*, Phys. Rev. B **69**, 014502 (2004).
[15] N. B. Christensen *et al.*, Phys. Rev. Lett. **93**, 147002 (2004).
[16] H. F. Fong *et al.*, Phys. Rev. B **61**, 14773 (2000).
[17] A. F. Barabanov *et al.*, JETP **92**, 677 (2001).
[18] A. M. Belemouk, A. F. Barabanov and L. A. Maksimov , Zh.Eksp.Teor.Fiz. **129**, 493 (2006) [JETP **102**, 431 (2006)].
[19] B. P. Stojkovic and D. Pines, Phys.Rev. B **55**, 8576 (1997).
[20] R. Hlubina, and T. M. Rice, Phys. Rev. B **51**, 9253 (1995).
[21] Y. Ando, S. Komiya, K. Segawa, S. Ono, Y. Kurita , Phys. Rev. Lett. **93**, 267001 (2004).